Dual-frequency GPS Precise Point Positioning with WADGPS Corrections

Hyunho Rho and Richard B. Langley
Department of Geodesy and Geomatics Engineering, University of New Brunswick, Fredericton, N.B. Canada

BIOGRAPHY

Hyunho Rho received an M.Sc. in 1999 in geomatics from Inha University, South Korea. He is currently a Ph.D. candidate in the Department of Geodesy and Geomatics Engineering at the University of New Brunswick (UNB), where he is investigating ways to improve ionospheric modeling for wide area differential GPS (WADGPS) and precise point positioning with WADGPS.

Richard Langley is a professor in the Department of Geodesy and Geomatics Engineering at UNB, where he has been teaching since 1981. He has a B.Sc. in applied physics from the University of Waterloo and a Ph.D. in experimental space science from York University, Toronto. Prof. Langley has been active in the development of GPS error models since the early 1980s and is a contributing editor and columnist for GPS World magazine. He is a fellow of the ION and shared the ION 2003 Burka Award.

ABSTRACT

A number of wide area differential GPS (WADGPS) services (e.g., WAAS, EGNOS, and CDGPS - the Canada-wide Differential GPS Service) are now in operation and more are planned for the future. These free services will enhance the availability of real-time DGPS corrections across countries and continents by providing a quality geo-referencing capability especially for single frequency L1 GPS users. However, the satellite orbit and clock WADGPS corrections can also be used to improve the GPS positioning accuracy for dual-frequency users.

The goal of the research described in this paper is the design of a GPS dual-frequency data processing technique capable of producing high-accuracy positioning results with WADGPS corrections.

In this paper, we have designed the forward carrier-phase smoothing technique in the measurement domain as an approach for implementing dual-frequency precise point positioning using WADGPS corrections. Results determined via developed software indicate that a few decimeter-level positioning accuracy is attainable at the 2D r.m.s. For these results, we didn't take into account the phase wind-up due to relative rotation of the satellite and receiver antennas, nor site displacement effects due to solid earth tides and ocean loading. To account for the satellite clock referencing issue, the effects of the satellite instrumental biases have been precisely investigated and the observation equations for the different observables assuming the source of corrections is WADGPS have been developed. With the developed observation model, we found about a 75 cm level of improvement in the horizontal position fixes and improvements of about factor of 2 in the vertical position component when the instrumental biases were correctly taken into account.

The presented results could serve as a baseline for further improvements to GPS single and dual-frequency precise point positioning with WADGPS corrections. Furthermore, the developed processing software can be used to monitor WADGPS performance anywhere in the service coverage area using observations from independent permanent networks. The receivers need not be equipped for WADGPS.

INTRODUCTION

A primary purpose of WADGPS is the provision of real-time DGPS corrections across countries and continents, providing a quality geo-referencing capability especially for single frequency L1 GPS users. However, the satellite orbit and clock WADGPS corrections can also be used to improve GPS positioning accuracy for dual-frequency users.

In general, both undifferenced carrier-phase and pseudorange measurements with precise ephemeris and clock data (such as those of the International GNSS Service) should be used to achieve the highest possible point-positioning accuracy [Heroux et al., 2001; Bisnath and Langley, 2001]. The sequential least squares and Kalman filter techniques are the common approaches used to mitigate the measurement noise and to achieve up to several centimeters positioning accuracy in post-

processing collected data. However, in contrast to post-processing with precise orbits and clocks, there are some special issues in using WADGPS corrections for dual frequency GPS point positioning. First, the position estimator should use a weighted least-squares approach with the epoch-by-epoch solution properly taking into account the uncertainty of each WADGPS correction at each epoch. In this case, the increased noise level by use of the ionosphere-free dual-frequency combination should be dealt with by a carrier-phase smoothing or filtering technique in the measurement domain. Second, as WADGPS services typically provide clock corrections which are referenced to the C1 (L1 C/A-code pseudorange) observable, there exist satellite clock referencing issues for the proper use of the corrections for dual-frequency observations. As long as satellite instrumental biases exist (C1 vs. P1 and P1 vs. P2), this issue should be properly reflected in the observation model.

In the following sections, our newly developed point positioning model with WADGPS corrections and carrier-phase smoothing method is discussed. Then we introduce a simple way to compute the P1-C1 bias at each station. A number of tests including checking for the P1-C1 bias effect and the overall performance of our developed models are discussed. Finally, conclusions and plans for future research are specified.

PRECISE POINT POSITIONING WITH WADGPS CORRECTIONS

Development of precise point positioning model with WADGPS corrections

Standalone Positioning Model

In general, we can write pseudorange observation equation as

$$P = \rho - dt_{ref} + dT_{ref} + I_{obs} + T + b^{s}_{obs-ref} + b^{r}_{obs-ref} + m_{obs} + e_{obs} \quad (1)$$

where P is the observed pseudorange, ρ is the geometric range between receiver and satellite, dt and dT are the satellite and receiver clock errors, respectively. I, T are the ionospheric and tropospheric delays and b^{s}, b^{r} satellite and receiver clock corrections, m is the multipath and e is the unmodelled error including receiver noise. All terms are expressed in meters and subscript "ref" indicates the reference for a correction and "obs" refers to the observable being used.

Specifically for the C1, P1 and P2 observables, we have

$$C1 = \rho - dt_{ref} + dT_{ref} + I_{C1} + T + b^{s}_{C1-ref} + b^{r}_{C1-ref} + m_{C1} + e_{C1}$$
$$P1 = \rho - dt_{ref} + dT_{ref} + I_{P1} + T + b^{s}_{P1-ref} + b^{r}_{C1-ref} + m_{P1} + e_{P1}$$
$$P2 = \rho - dt_{ref} + dT_{ref} + I_{P2} + T + b^{s}_{P2-ref} + b^{r}_{P2-ref} + m_{P2} + e_{P2}$$

Point Positioning Using the Navigation Message only

The satellite instrumental biases depend on the satellite clock reference used. Consider first, only applying the "L1-L2 correction", T_{GD}, as given in the broadcast navigation message. This gives a clock referenced to the P1P2 ionosphere-free linear combination. If we apply the T_{GD} clock correction to the satellite clock correction, as instructed in ICD GPS 200, we get the clock referenced to P1. T_{GD} is related to the P1P2 interfrequency instrumental delay, b^{S}_{P1-P2} as follows:

$$T_{GD} = \frac{1}{1-\gamma} b^{S}_{P1-P2} \text{ where } \gamma = \frac{f_1^2}{f_2^2}$$

and f_1 and f_2 are the L1 and L2 carrier frequencies respectively.

Using the P1P2 clock reference, we have

$$C1 = \rho - (dt_{P1P2} - T_{GD}) + dT_{ref} + I_{C1} + T + b^{s}_{C1-P1} + b^{r}_{C1-ref} + m_{C1} + e_{C1}$$
$$P1 = \rho - (dt_{P1P2} - T_{GD}) + dT_{ref} + I_{P1} + T + b^{s}_{P1-P1} + b^{r}_{P1-ref} + m_{P1} + e_{P1}$$
$$P2 = \rho - (dt_{P1P2} - T_{GD}) + dT_{ref} + I_{P2} + T + b^{s}_{P2-P1} + b^{r}_{P2-ref} + m_{P2} + e_{P2}$$

Note that the satellite bias term for P1 is zero and that the bias for P2 is related to T_{GD} as follows:

$$b^{s}_{P2-P1} = (\gamma - 1) T_{GD}$$

So, the equation for P2 can also be written as

$$P_2 = \rho - (dt_{P1P2} - T_{GD}) + dT_{ref} + I_{P2} + T + (\gamma - 1) T_{GD} + b^{r}_{P2-ref} + m_{P2} + e_{P2}$$
$$= \rho - (dt_{P1P2} - \gamma T_{GD}) + dT_{ref} + I_{P2} + T + b^{r}_{P2-ref} + m_{P2} + e_{P2}$$

Consider the C1P2 ionosphere-free linear combination, ignoring the receiver biases, multipath, and noise:

$$\alpha C1 - \beta P2 = \rho - (dt_{P1P2} - \alpha T_{GD} + \beta\gamma T_{GD}) + dT_{ref} + T + \alpha b^{S}_{C1-P1}$$

where

$$\alpha = \frac{f_1^2}{f_1^2 - f_2^2} \cong 2.546 \,,\ \beta = \frac{f_2^2}{f_1^2 - f_2^2} \cong 1.546$$

Noting that $\gamma = \frac{\alpha}{\beta}$,

we have

$$\alpha C1 - \beta P2 = \rho - dt_{P1P2} + dT_{ref} + T + \alpha b^{S}_{C1-P1}$$

WADGPS Positioning Model

Now, consider satellite clock corrections from WAAS or CDGPS. These clock corrections are referred to C1 and

are in addition to the navigation message corrections. We have, therefore

$$C1 = \rho - (dt_{P1P2} - T_{GD} + \delta t_{C1}) + dT_{ref} + I_{C1} + T + b^{S}_{C1-C1} + b^{r}_{C1-ref} + m_{C1} + e_{C1}$$
$$= \rho - (dt_{P1P2} - T_{GD} + \delta t_{C1}) + dT_{ref} + I_{C1} + T + b^{r}_{C1-ref} + m_{C1} + e_{C1}$$

where δt_{C1} is the WADGPS clock correction. Note that T_{GD} is applied but no other satellite-bias correction is needed.

Continuing with the P1 and P2 observables, we have

$$P1 = \rho - (dt_{P1P2} - T_{GD} + \delta t_{C1}) + dT_{ref} + I_{P1} + T + b^{s}_{P1-C1} + b^{r}_{P1-ref} + m_{P1} + e_{P1}$$
$$P2 = \rho - (dt_{P1P2} - T_{GD} + \delta t_{C1}) + dT_{ref} + I_{P2} + T + b^{s}_{P2-C1} + b^{r}_{P2-ref} + m_{P2} + e_{P2}$$

The bias $b^{s}_{P2-C1} = b^{s}_{P2-P1} + b^{s}_{P1-C1} = (\gamma - 1)T_{GD} + b^{s}_{P1-C1}$

So, we have for P2

$$P2 = \rho - (dt_{P1P2} - T_{GD} + \delta t_{C1}) + dT_{ref} + I_{P2} + T + (\gamma - 1)T_{GD} + b^{s}_{P1-C1} + b^{r}_{P2-ref} + m_{P2} + e_{P2}$$
$$= \rho - (dt_{P1P2} - \gamma T_{GD} + \delta t_{C1}) + dT_{ref} + I_{P2} + T + b^{s}_{P1-C1} + b^{r}_{P2-ref} + m_{P2} + e_{P2}$$

The ionosphere-free linear combination using the WADGPS correction is (ignoring the receiver bias, multipath, and noise terms)

$$\alpha C1 - \beta P2 = \rho - (dt_{P1P2} - \alpha T_{GD} + \beta\gamma T_{GD} + \delta t_{C1}) + dT_{ref} + T - \beta b^{S}_{P1-C1}$$
$$= \rho - (dt_{P1P2} + \delta t_{C1}) + dT_{ref} + T - \beta b^{S}_{P1-C1} \qquad (2)$$

So, for the C1P2 combination with WADGPS clock corrections, T_{GD} is not applied but b^{s}_{P1-C1} should be applied with the factor $\beta = 1.546$.

Modified Hatch Type Smoothing Algorithm for WADGPS

With the WADGPS corrections for dual frequency GPS point positioning, the increased noise level by use of the ionosphere-free combination (see eqn.2) should be properly handled. As long as the position estimator should use a weighted least-squares approach with epoch-by-epoch solution properly taking into account the uncertainty of each WADGPS correction at each epoch, the smoothing process needs to generate an uncertainty for each smoothed measurement in the measurement domain.

A position domain smoothing method has been proposed [Bisnath and Langley, 2001]. The advantage of this approach is that it is not significantly affected by a change of satellite constellation as long as more than four satellites are observed at the current epoch. However the position domain solution may have a transient as the solution bias switches from one state to another with the source of differential corrections changed [McGraw et al., 2005].

In this paper, we introduce a modified Hatch type filter to properly use the WADGPS corrections. The basic form can be attributed to the carrier-phase smoothing algorithm which was first introduced by Hatch [1982]. This filter is effective if the change in carrier-phase and pseudorange can be considered to be equal over a certain interval.

The main idea of our modification is to get the uncertainty of the smoothed pseudorange. we consider both systematic and random error effects by analyzing the error propagation of different error sources for the smoothed pseudorange. As long as WADGPS provides the satellite orbit, clock and ionospheric delay (for the single frequency case) corrections with their uncertainties, the systematic errors and their residual effects can be properly managed.

To mitigate random error, multipath and noise effects, a set of noise model coefficient are used. McGraw et al. [2000] describe the multipath and noise level for different qualities of receivers and provided the estimated coefficients for the exponential noise model. Their work was originally carried out for the Local Area Augmentation System (LAAS) but is generally applicable.

The combined multipath and noise in the GPS measurements can be modeled by using a tuned exponential function at each station. However, we try to mimic the real-time situation by use of the above noise model with the WADGPS corrections.

A Modified Carrier-phase Smoothed Pseudorange Algorithm

Consider a series of n observations of pseudoranges P_k and its variance: $D^2_{P_k}$, carrier ranges: Φ_k and its variance $D^2_{\Phi_k}$, k = 1 , .. , i.

The general GPS observation equations for pseudorange and carrier phase are:

$$P_k = \rho_k + (dt - dT) + d_{orb} + T + I + m_k + e_k$$
$$\Phi_k = \rho_k + (dt - dT) + d_{orb} + T - I + N\lambda + M_k + \varepsilon_k \qquad (3)$$

where d_{orb} is the orbit error, N is the carrier phase ambiguity, M is the multipath error for carrier phase and ε is the carrier phase noise. The other terms have their usual meaning as we described in equation (1) and again, all terms are expressed in meters.

Then we can form the weighted forward smoothing model:

$$\overline{P}_i = \sum_{k=1}^{i} W_k (P_k + \Phi_i - \Phi_k) / \sum_{k=1}^{i} W_k$$

and the equivalent recursive form is:

$$\overline{P_i} = \frac{W_i}{\sum_{k=1}^{i} W_k} P_i + \frac{\sum_{k=1}^{i} W_k - W_i}{\sum_{k=1}^{i} W_k} (\overline{P}_{i-1} + \Phi_i - \Phi_{i-1}) \qquad (4)$$

$$\overline{P_1} = P_1$$

where, $\overline{P}_i$ is the smoothed pseudorange upto ith epoch and W_k is the weight for the raw pseudorange.

Due to the opposite signs of the ionospheric delay terms between pseudorange and carrier phase (see eqn 3), we can see twice the ionospheric delay change, the so called divergence, in equation (4). The smoothing interval for single frequency use is limited by this divergence factor (see, e.g., Kee et al., [1997] and MacGraw et al., [2005]).

For the dual-frequency case, the ionosphere-free pseudorange and carrier-phase can be formed as:

$$\begin{aligned} P_{IF} &= \alpha C1 - \beta P2 \\ &= \rho + (dt - dT) + d_{orb} + T + \alpha(e_{C1} + m_{C1}) - \beta(e_{P2} + m_{P2}) \\ \Phi_{IF} &= \alpha\Phi 1 - \beta\Phi 2 \\ &= \rho + (dt - dT) + d_{orb} + T + \alpha N_{\Phi 1} - \beta N_{\Phi 2} + \alpha(\varepsilon_{\Phi 1} + M_{\Phi 1}) - \beta(\varepsilon_{\Phi 2} + M_{\Phi 2}) \end{aligned} \qquad (5)$$

we assumed the carrier-phase ambiguities, $N_{\Phi 1}$ and $N_{\Phi 2}$, are constants.

Now, the pseudorange and carrier changes in time can be written:

$$\begin{aligned} \Delta P_{IF} &= -\Delta dT + \Delta d_{orb} + \Delta T + \alpha(\Delta e_{C1} + \Delta m_{C1}) - \beta(\Delta e_{P2} + \Delta m_{P2}) \\ \Delta\Phi_{IF} &= -\Delta dT + \Delta d_{orb} + \Delta T + \alpha(\Delta\varepsilon_{\Phi 1} + \Delta M_{\Phi 1}) - \beta(\Delta\varepsilon_{\Phi 2} + \Delta M_{\Phi 2}) \end{aligned} \qquad (6)$$

Equation (6) shows that first, there is no divergence problem as with single-frequency observations and second, we are satisfied with the condition that the change in carrier phase and pseudorange are nominally equal. As long as the noise and multipath in carrier phase is much smaller than that of pseudorange, the certain portion of differences between carrier phase and pseudorange can be averaged out within a certain time interval.

Equations (3) and (6) include some biases which slowly change with time, i.e., residual satellite orbit, clock and troposphere effects. Within a certain time interval, those long-term biases are not averaged out with a smoothing process. However with the WADGPS corrections, we have satellite orbit and clock corrections with their uncertainties. We also used the UNB3 troposphere model with Niell mapping function as well as its uncertainty to mitigate the tropospheric errors in the observables [Collins and Langley, 1999]. The only difference in the troposphere model compared to that currently used by WAAS and CDGPS was that we used the Niell mapping functions rather than that of Black and Eisner [WAAS MOPS, 1999].

So now we can deal with much smaller residual errors for the long-term biases in our observations. To get a maximum advantage of precise carrier phase, we didn't use a specific smoothing interval (for the results shown later) in this paper. The only limitation which we considered was cycle slips. If a cycle slip happened in the carrier phase, we reset the smoothing process.

However we should mention that this setup is only for the static process with a geodetic quality receiver and chock-ring antenna. In the kinematic case, the smoothing interval should be properly decided.

Weighting scheme for smoothing process

Let the uncertainty caused by white noise and multipath be σ, and the uncertainty caused by satellite orbit, clock, and atmosphere delay, Γ. Then we can get,

$$D_{P_i}^2 = \sigma_{P_i}^2 + \Gamma_i^2$$

From equation (3) and (6),

$$\Gamma_i = \left[(S_1 \cdot \delta T)^2 + \delta I^2 + \cdot \delta_{dT_i}{}^2\right]^{1/2}$$

where, S_1 is the scale factor to count on a tropospheric delay residual, corresponding to δT. S_1 can be assigned an empirical value of 0.01 for the UNB3 tropospheric model. δI is the uncertainty for the ionospheric correction (single frequency case) from WADGPS, δ_{dT} is the uncertainty for satellite orbit and clock from WADGPS.

The systematic errors are same for pseudorange and carrier phase:

$$\Gamma_{\Phi_i} = \Gamma_{P_i} = \Gamma_i$$

To get an estimate of the random errors, σ, we used the coefficients of the exponential noise function for a geodetic quality receiver [McGraw et al., 2000]:

$$\sigma_{P_i} = a_0 + a_1 \cdot \exp(-\theta_i / \theta_c)$$

$$a_0 = 0.16$$

$$a_1 = 1.07$$

$$\theta_c = 15.5(\text{deg})$$

where θ_i : elevation angle in degrees

Finally, the weight for the raw pseudorange is:

$$W_i = 1 / D_{P_i}^2$$

So we used above W_i for the weight in the equation (4).

To get the uncertainty for smoothed pseudorange

By use of equation (4), we can get the random error for smoothed pseudorange:

$$\sigma_{\bar{P}_i}^2 = \left(\frac{W_i}{\sum_{k=1}^{i} W_k}\right)^2 \sigma_{P_i}^2 + \left(\frac{\sum_{k=1}^{i} W_k - W_i}{\sum_{k=1}^{i} W_k}\right)^2 \sigma_{\bar{P}_{i-1}}^2 + \left(\frac{\sum_{k=1}^{i} W_k - W_i}{\sum_{k=1}^{i} W_k}\right)^2 (\sigma_{\Phi_i}^2 + \sigma_{\Phi_{i-1}}^2)$$

$$\sigma_{\bar{P}_i}^2 \approx \left(\frac{W_i}{\sum_{k=1}^{i} W_k}\right)^2 \sigma_{P_i}^2 + \left(\frac{\sum_{k=1}^{i} W_k - W_i}{\sum_{k=1}^{i} W_k}\right)^2 \sigma_{\bar{P}_{i-1}}^2$$

For the ionosphere-free combination, from our analysis for the noise level of C1 code and P2 code, we can suppose $\sigma_{P_{f1}} = \sigma_{P_{f2}} = \sigma_P$, then,

$$\sigma_{P_{IF_i}}^2 = (\alpha_1^2 - \beta_1^2)\sigma_{P_i}^2$$

and,

$$\Gamma_{IF_i} = \left[(S_1 \cdot \delta T)^2 + (\delta_{dT})^2\right]^{1/2}$$

and again, the systematic errors are same for pseudorange and carrier phase:

$$\Gamma_{\Phi_{IF_i}} = \Gamma_{P_{IF_i}} = \Gamma_{IF_i}$$

$$\Gamma_{\bar{P}_{IF_i}} = \Gamma_{\Phi_{IF_i}} = \Gamma_{IF\,i}$$

So finally we have an uncertainty for smoothed pseudoranges which considers both systematic and random error effects:

$$D_{\bar{P}_i}^2 = \sigma_{\bar{P}_i}^2 + \Gamma_{\bar{P}_i}^2$$

The receiver position is finally calculated by weighted least-squares with the smoothed pseudoranges and the following weighting scheme.

$$W_{\bar{P}_i} = 1 / D_{\bar{P}_i}^2$$

EVALUATION

To have CDGPS and WAAS corrected positioning solutions for analysis, we used the extended UNB RTCA/MRTCA correction software for dual frequency data. A more detailed explanation of the previous version of software (single frequency case) can be found in Rho et al. [2003]. In general, there is no difference between the extended and previous software versions except we used the developed observation model and smoothing algorithm for the dual frequency case as described in this paper. Since the WAAS and CDGPS binary data stream corrections have been archived at UNB on daily basis from the middle of 2001 for WAAS and 2003 for CDGPS, we used data from those archives for our analyses.

Data Description

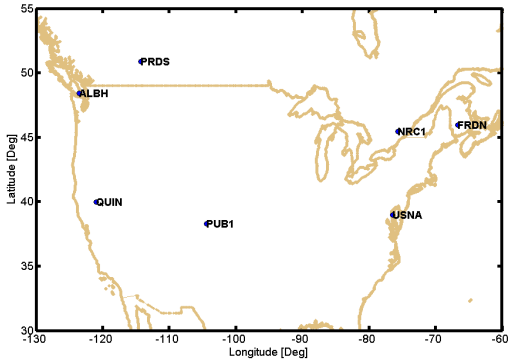

Figure 1. The 7 selected reference stations

For analyses conducted using the developed method for both single and dual-frequency positioning results, we selected 7 stations: four stations from the Canadian Active Control System (CACS) network and the other three stations from the International GNSS service (IGS) network in the U.S.A. (see Figure 1). The location and receiver type of the selected stations are listed in Table1.

Table1. Specification of the stations and receivers

Station	Location	Receiver
ALBH	Victoria, BC, CANADA	AOA BenchMark ACT
PRDS	Calgary, ALTA, CANADA	AOA SNR-12 ACT
NRC1	Ottawa, ONT, CANADA	AOA SNR-12 ACT
FRDN	Fredericton, NB, CANADA	AOA BenchMark ACT
QUIN	Quincy, CA, USA	Ashtech UZ-12
PUB1	Pueblo, CO, USA	Ashtech Z-XII3
USNA	Annapolis, MD, USA	Ashtech UZ-12

To see if there are certain un-modeled ionospheric effects reflected in the positioning results on an ionospheric storm day, we selected two sample days. On November 10 (day of year (DOY): 315), 2004, there was a significant geomagnetic disturbance. We choose this day as a significant ionospheric storm day. November 17 (DOY: 322), 2004 was selected as an ionospheric quiet day. Figure 2 shows the disturbance storm time (Dst) index and Kp index. The more negative the Dst values the more intense the geomagnetic disturbance. We also used the Kp index for confirmation. A significant geomagnetic disturbance occurred for almost all day (Kp>5) on November 10 (DOY 315), 2004.

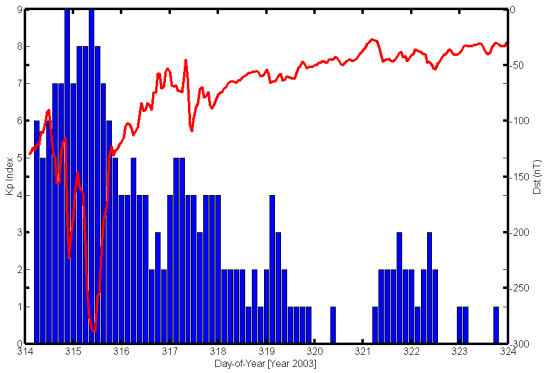

Figure 2. Dst and Kp indices from November 14 to November 18, 2004. The blue bar shows the three-hour Kp index and the solid line (red) shows the Dst index.

Satellite Orbits and Clocks

To evaluate the WADGPS orbit correction accuracy for two sample days, we determined the accuracy of the broadcast orbits as well as the orbit after WADGPS corrections. To generate the statistics for all satellites for each day, the broadcast ephemeredes from Scripps Orbit and Permanent Array Center (SOPAC) were used. SOPAC provides the daily GPS observation data as well as navigation files, retrieved from identified global core observatories. Since the CDGPS orbit corrections are generated in the NAD83 (CSRS) reference frame, the final precise ephemeredes from NRCan GSD were used as truth for the CDGPS analyses [NRCan GSD, 2005]. To evaluate the broadcast and WAAS orbit accuracy, the final precise ephemeredes from IGS were used as truth.

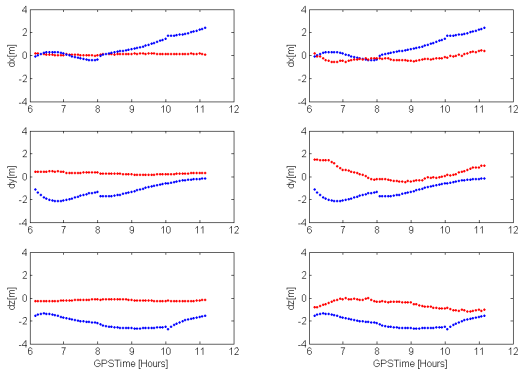

Figure 3. Example of the WADGPS-corrected satellite orbit errors. Left panels show the CDGPS-corrected satellite orbit error and the right panels show of the WAAS-corrected satellite orbit error for PRN21 on November 10, 2004. Blue dots represent the broadcast orbit errors and red dots show the WADGPS-corrected orbit errors.

Figure 3 shows that generally the errors in the broadcast orbit were well corrected by applying both CDGPS and WAAS orbit corrections. However the CDGPS-corrected orbits have smaller variations than WAAS-corrected orbits. This might be explained by the fact that corrections to the GPS broadcast orbits in CDGPS are determined using orbital predictions based on GPS global solutions [CDGPS ICD, 2003].

Table 2. Summary for CDGPS and WAAS orbit errors in Radial (dR), along track (dS) and cross track (dW).

Unit: meters	WAAS [315]	CDGPS [315]	WAAS [322]	CDGPS [322]
3d rms	1.308	0.870	1.565	0.888
Mean[dR]	-0.200	-0.483	-0.261	-0.506
Mean[dS]	0.112	-0.137	0.215	-0.123
mean[dW]	0.059	-0.065	0.084	-0.081
Rms[dR]	0.523	0.668	0.741	0.697
Rms[dS]	0.985	0.299	1.039	0.311
Rms[dW]	0.708	0.264	0.918	0.256

Table 2 shows the overall 3d root-mean-square (r.m.s) error for both CDGPS- and WAAS-corrected orbits for our two sample days. Based on our analysis with limited two sample days data, the CDGPS orbit accuracies were a bit better than those of WAAS in terms of 3d r.m.s. error. The computed 3d r.m.s. WAAS errors are comparable with the 1.3 m in 3d r.m.s. reported by Zhang and Bartone [2005]. However, Table 2 also shows orbit errors of both systems are comparable in terms of radial component of errors.

A more detailed explanation for WADGPS corrected orbits and their errors is given by Rho and Langley [2003] for CDGPS and Zhang and Bartone [2005] for WAAS.

Satellite P1-C1 Bias Effects in Precise Point Positioning

The different signal path delay for different signal components gives rise to satellite and receiver instrumental biases, the so-called P1-P2 and P1-C1 differential code biases (DCB). In general, the satellite P1-P2 DCBs vary between ±4 nanoseconds and about ±2 nanoseconds for P1-C1 DCBs. If we assume the receiver DCBs are common for all satellites at a single station, we can simply assume the receiver biases are absorbed by the receiver clock error in the estimation. In this case, we are not counting on a variation of receiver biases, even if there might exist a temporal variation of receiver biases caused by several factors including the surrounding local temperature conditions [Chao et al., 1996].

The above derived equation (2) shows that the P1-C1 bias should be considered as a source of error with a corresponding scale factor when we use the WADGPS corrections. To properly take into account for a P1-C1 bias into the WADGPS observation model, there are three methods available for use. First we can simply use a CODE (Center for Orbit Determination in Europe) P1-C1

table for the corrections. However the P1-C1 table from CODE consists of monthly averaged values so they might not be sensitive to any daily P1-C1 bias variation. Second, if the receiver provides all three C1, P1 and P2 observables, we can directly generate a P2', P2' = C1 + (P2-P1) observable and use it. This P2' observable can reflect a temporal variation of the P1-C1 bias but additional noise is introduced. However, Gao et al. [2001] modeled satellite P1-C1 biases and showed there are constant and time variant. Third, we can compute the P1-C1 bias at each station by use of P1-C1 observables directly from the receiver. If the dominant source of P1-C1 bias is a constant type, this method will work well. However if there is a significant variation in the P1-C1 bias during the day, this method and the CODE table approach might be not be the best ways to handle the P1-C1 bias.

$$P1-C1=(b^{r}_{P1}-b^{r}_{C1})+(b^{s}_{P1}-b^{s}_{C1})+(m_{P1}-m_{C1})+(e_{P1}-e_{C1}) \quad (7)$$

To calculate the variation of satellite P1-C1 DCB at the station, the P1-C1 time series were generated for the all monitored satellites for the whole day. The above equation (7) shows the P1-C1 time series behaves as a function of satellite and receiver P1-C1 biases and residual multipath and noise. In this paper, the selected 7 stations have chock-ring antennas. With a chock-ring antenna, the residual multipath in P1-C1 is largely eliminated. And the residual noise behaves randomly. The remaining terms in the expression for P1-C1 are just the P1-C1 bias for satellite and receiver.

The following Figure 4 illustrates the P1-C1 biases at station NRC1 on November 17, 2004.

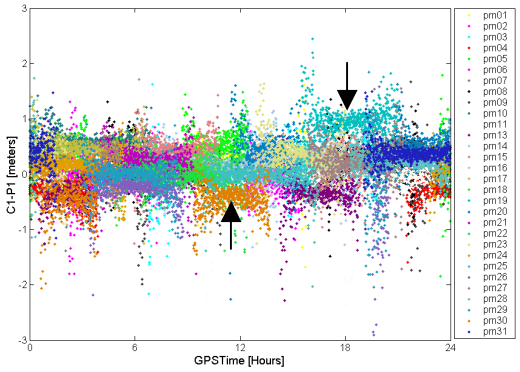

Figure 4. P1-C1 time series for each satellite at station NRC on November 17, 2004.

Figure 4 clearly shows the P1-C1 values include elevation dependent multipath and noise effects. And we can also see that the P1-C1 bias is sometimes varying with time, with a drift or some other time variation (see the black arrow in Figure 4). However we can see there exist different biases for different satellites.

To complete the equation to compute the P1-C1 bias at the station, we made another assumption that the receiver P1-C1 bias is constant for at least one day. To compute the satellite and receiver combined P1-C1 bias, we take the mean of all P1-C1 biases using data available over time. We then compute the mean of the biases separately for each satellite. The bias for satellite i is then given by:

$$SAT\_Bias_i = \overline{Bias_i} - \overline{Bias_{1-31}} \quad (8)$$

To get the daily mean of each satellite P1-C1 bias, all the P1-C1 biases for each satellite from the seven stations were averaged.

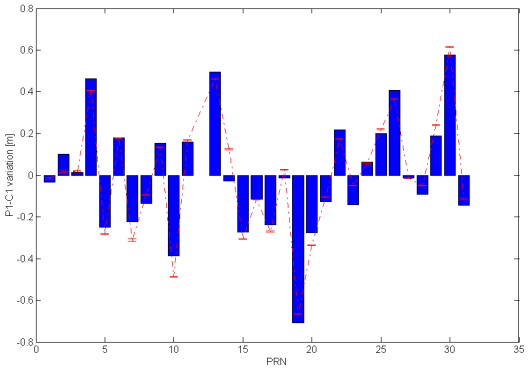

Figure 5. Comparison of P1-C1 DCBs using the UNB approach, the mean of C1-P1 biases from the seven stations, (blue bar) on November 17, 2004 and CODE's monthly mean (red dashed-line with dot) for November 2004.

In Figure 5, there exist some discrepancies between our daily mean of seven stations and the monthly mean values from CODE. The maximum difference in terms of absolute discrepancies was 15 cm for satellite PRN 14 for this day. The standard deviation of the discrepancies was about 3.4 cm. The differences might be explained by the different number of stations which contributed for the computation for the P1-C1 bias at UNB and CODE. CODE actually used about 30-40 stations to compute the satellite P1-C1 biases [CODE, 2005]. Figure 5 also shows the peak-to-peak variation of satellite P1-C1 bias was about ± 60 cm, except for PRN 19 from our calculation. This value is reasonable, as compared with the maximum values in Gao et al. [2001].

Sensitivity Test

To decide the overall processing scheme with specific type of correction for P1-C1 bias, we selected the NRC1 station for the sensitivity test and used four different types of P1-C1 corrections. The NRC1 station was selected because we saw there was a biggest improvement in terms of positioning accuracy with our approach.

For the different type of corrections, first we used the P1 and C1 observables to generate P2' observable and second we used the estimated P1-C1 biases which we computed at the NRC1 station. We also used mean of P1-C1 of all seven stations and finally used the P1-C1 bias table from CODE. The following table shows the statistics of the positioning results with the four different types of corrections.

Table 3. Statistics for the dual-frequency CDGPS point positioning results with four different types of corrections at station NRC1

[m]	P2'	UNB P1-C1 (NRC1)	UNB P1-C1 (all stns.)	CODE Table
95% Horiz.	0.315	0.445	0.477	0.535
95% Vert.	0.551	0.605	0.643	0.957
Bias N	0.013	0.000	-0.002	0.006
Bias E	-0.037	-0.039	-0.045	-0.050
Bias U	-0.024	-0.085	-0.093	-0.139

Table 3 shows the best results in the positioning domain were achieved when we used the P1 and C1 observables to generate the P2' observable. The only difference in this approach compared to the other three approaches, is that we could accommodate a temporal variation of P1-C1 biases even though the noise level increased. The statistics might show the time variation is more significant than the increased noise level at station NRC1. The second and third best performance was when we used a computed P1-C1 bias set directly at the station and when we used a set of daily mean from all seven stations. This represents the local sensitivity and indicates that daily variations are more significant than the overall mean of constant variations for P1-C1 bias from CODE at this station. And the table also shows the P1-C1 biases have more bias effective or the height component rather than horizontal components (see bias in height components).

We used the P2' approach for the entire process with 7 stations taking into account the P1-C1 bias for the two days of our analysis.

There is another good advantage to using P2' approach. Since the WADGPS corrections are designed to be used in a real-time, the P2' approach is the most useful way to handle the P1-C1 bias as the receiver can generate all the necessary measurements to make P2'. The other three approaches for the corrections cannot be used in a real-time fashion as long as we need to wait some time to compute or get the P1-C1 bias at UNB or from CODE.

P1-C1 Bias Effects in Point Positioning

The following Figure 6 shows the P1-C1 bias behavior in the GPS point positioning. In Figure 6, the characteristic of the P1-C1 bias looks to be not constant but varying with time. This is because more than 4 satellites are used to estimate the receiver position. The different signs and magnitudes of variations for P1-C1 biases of satellites are combined together for the position estimation. However, we can clearly see the improvements when we properly take into account the bias effect in the model.

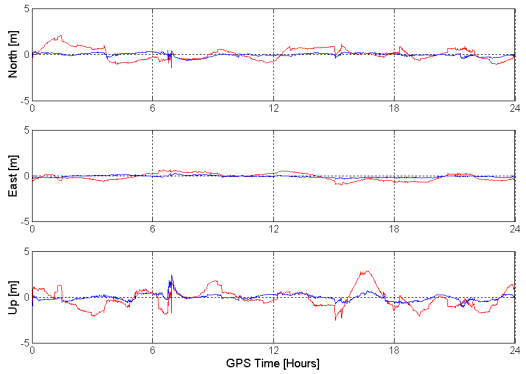

Figure 6. P1-C1 bias effects to the positioning results at NRC1 station on November 17, 2004. The color, red shows the biased solution (bias correction not applied) and blue represents unbiased solution (correction applied).

Figure 6 also shows most improvements occur for the up component and there exists a long term variation but overall, the one day mean is not so much biased.

To see the overall effects of the P1-C1 biases in the positioning domain, we generate the differences between biased and unbiased solutions at all seven stations. The solution was compiled by using the smoothed ionosphere-free results with WAAS or CDGPS orbit and clock corrections as appropriate.

Table 4. Statistics of the differences between P1-C1 biased and unbiased solutions using all seven stations on November 17, 2004.

Difference [m]	Mean
95% Horiz.	0.750
95% Vert.	1.410
Bias N	0.056
Bias E	-0.003
Bias U	-0.104

Table 4 shows the most significant improvement occurs in the height component where the bias is about 10 cm. The statistics also shows 0.75 meters of improvement in the scatter of the horizontal component and about 1.4 meters improvement in the vertical sactter. This statistics shows that the P1-C1 bias issue is significant for dual-frequency point positioning with WADGPS corrections.

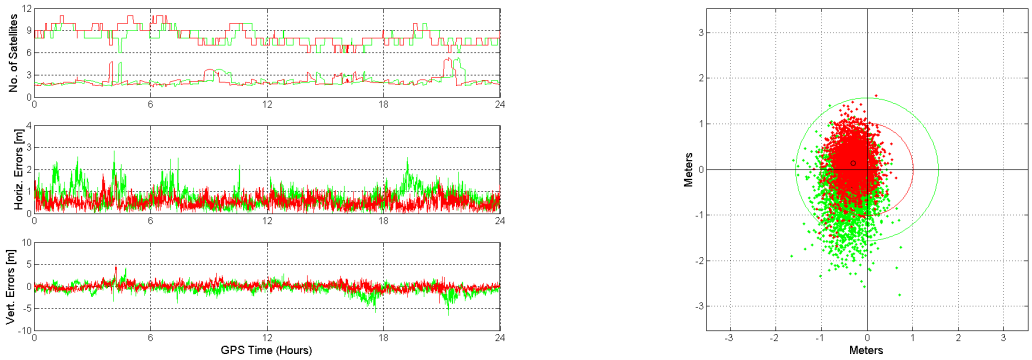

Figure 7: Point positioning results from single frequency (C1, not smoothed) with CDGPS corrections at the station NRC1. Green: ionospheric storm day, November 10, 2004, red: ionospheric quiet day, November 17, 2004. The upper panel of the time series on the left shows the number of satellites and PDOP. Note the overall biases in the solutions.

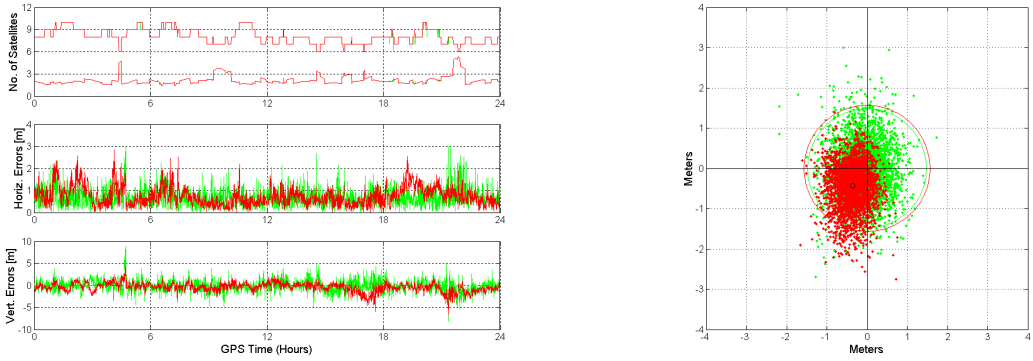

Figure 8: Point positioning results with CDGPS corrections at station NRC1 on a storm day, November 10, 2004. Green: the results from the ionosphere-free combination without smoothing and red: the results from the single frequency analysis (C1, not smoothed).

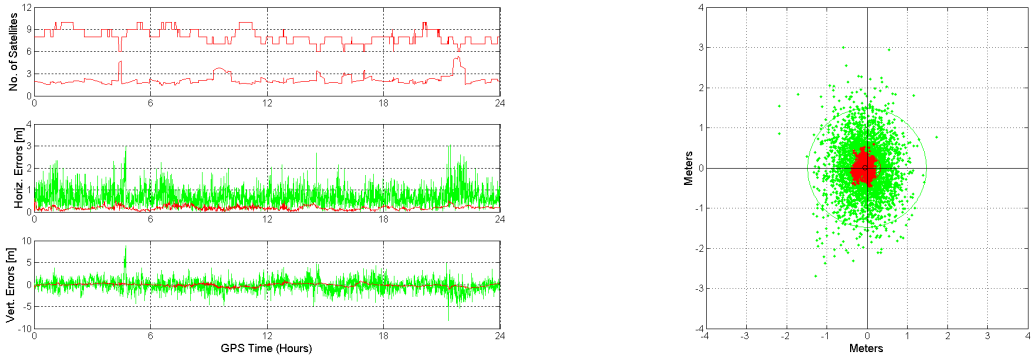

Figure 9: Point positioning results with CDGPS corrections at the station NRC1 on a storm day, November 10, 2004. Green: dual-frequency ionosphere-free combination without smoothing, red: dual frequency ionosphere-free combination with smoothing.

Table 5. Statistics for the point positioning process with CDGPS corrections at station NRC1, IF represents the ionosphere-free combination used, No-SM means the solution without smoothing process

Unit: meters		95% Horiz.	95% Vert.	Bias N	Bias E	Bias H
NRC1 station CDGPS	C1 (322)	1.011	1.443	0.133	-0.306	0.027
	C1 (315)	1.561	2.332	-0.437	-0.363	-0.431
	IF No-SM (315)	1.476	2.753	0.006	-0.052	-0.174
	IF SM (315)	0.337	0.659	0.012	-0.044	-0.091

Data Testing and Analysis

In order to clearly see what can be improved with our newly developed methods, the point positioning process with three scenarios was carried out with the NRC1 data. We used the storm day, November 10, 2004, to see more about the ionospheric storm effects especially for the single-frequency case. The three scenarios are first, the single frequency point positioning with CDGPS corrections for both ionospheric quiet and storm days. We also processed the data.

With the ionosphere-free combination but without smoothing. The purpose is to see the increased noise effects in the positioning domain. And finally we processed the ionosphere-free combination with the developed smoothing method.

In Figure 7, the time series (left panel) shows the positioning results are noisier when the ionospheric storm happened compared to when the ionosphere was quiet. The 95% accuracies were degraded about 0.55 m in the horizontal and about 1.9 m in the vertical components. We also can see the biases in north, east and up components are increased compared with an ionospheric quiet day. However, we can also see that biases exist in the north and east components even when the ionosphere was quiet. It might show there exists some residual errors for the satellite orbit, clock and ionosphere corrections, which were not well corrected by CDGPS correction for November 15, 2004. We will see later that those biases also happened with the WAAS corrections (see Table 6) for this day. It shows WAAS also had some difficulties in modeling the satellite orbit and clock on November 17, 2004.

In Figure 8, we can see the biases are dramatically reduced by using an ionosphere-free combination. However, the positioning accuracy with the ionosphere-free solution but without smoothing, was significantly degraded compared to the single-frequency case especially for the vertical component. It is clear that the increased noise level by use of the ionosphere-free combination with the P2' observable significantly degraded the positioning accuracy. However, the errors which are caused by significant ionospheric variations are reasonably well removed (see the time series of Figure 8). Finally, Figure 9 shows our smoothing algorithm properly worked in the measurement domain, improving the 95% positional accuracy by more than 1 m in the horizontal component and about 2 m in the vertical.

To see the daily mean differences between the ionospheric quiet day and storm day, we took a mean of the 95% horizontal and vertical errors from Table 6. To separate CDGPS and WAAS corrected solutions, the results from the first four stations, ALBH, PRDS, NRC1 and FRDN, were used to represent CDGPS performance and the other three stations were used to represent WAAS performance. With the single frequency observable on the ionospheric quiet day, the point positioning results with CDGPS corrections achieved about 0.96m as the mean of the 95% horizontal errors and 1.30m as the mean of the 95% vertical error. With the WAAS corrections, it was about 1.0m for the mean of the 95% horizontal error and 1.46m for the mean of the 95% vertical error. The statistics for WAAS and CDGPS performance are comparable on the ionospheric quiet day.

Table 6. Statistics for the point positioning results for all seven stations by use of CDGPS (ALBH, PRDS, NRC1 and FRDN) and WAAS (QUIN, PUB1 and USNA) corrections. [Unit: meters].

Stations	Observables	315,November 10, 2004, Ionospheric storm day					322, November 15, 2004, Ionospheric quite day				
		95% Horiz	95% Vert.	Bias N	Bias E	Bias H	95% Horiz	95% Vert.	Bias N	Bias E	Bias H
ALBH	C1	0.991	1.519	-0.187	-0.083	0.160	0.967	1.239	0.297	-0.078	0.091
	IF SM	0.503	0.878	0.041	-0.084	-0.038	0.576	0.737	0.025	-0.108	-0.050
PRDS	C1	1.251	2.027	-0.010	-0.028	0.198	0.957	1.262	0.220	0.029	0.232
	IF SM	0.655	0.938	0.040	-0.084	0.154	0.523	0.872	0.063	-0.070	0.135
NRC1	C1	1.561	2.332	-0.437	-0.363	-0.431	1.011	1.440	0.133	-0.306	0.027
	IF SM	0.337	0.659	0.012	-0.044	-0.091	0.315	0.551	0.013	-0.037	-0.024
FRDN	C1	1.657	2.550	-0.321	-0.285	-0.605	0.906	1.273	0.362	-0.188	-0.385
	IF SM	0.385	0.619	0.061	-0.064	-0.194	0.334	0.668	0.025	-0.032	-0.114
QUIN	C1	0.913	1.889	0.002	-0.004	-0.227	0.954	1.476	0.315	0.128	-0.078
	IF SM	0.606	1.442	-0.002	0.010	-0.032	0.635	1.125	0.05	0.014	-0.042
PUB1	C1	0.876	2.054	-0.124	-0.079	-0.353	0.953	1.652	0.185	-0.118	0.099
	IF SM	0.553	1.349	-0.021	-0.039	-0.14	0.630	1.332	-0.05	-0.144	0.029
USNA	C1	1.269	2.457	-0.203	0.082	-0.485	1.223	2.082	0.152	-0.098	-0.048
	IF SM	0.768	1.338	-0.044	-0.008	-0.288	0.882	1.412	-0.042	-0.063	-0.150

However, when the ionospheric storm happened, the mean of the 95% horizontal errors degraded about 40cm and the mean of the 95% vertical error degraded about 80 cm. However, interestingly, with the WAAS corrections, there was about 16cm improvement in the 95% horizontal error even though there was about 65cm degradation in the mean of the 95% vertical errors when the ionosphere was significantly disturbed. One possible explanation is that there was about 26cm improvements in the 3d r.m.s. (see Table 2) for WAAS orbit accuracy compared with the quiet day.

By use of the smoothing process with the ionosphere-free combination, there was about 52cm improvement compared with the C1 only solution in the mean of the 95% horizontal error with CDGPS corrections. And there was about 36 cm improvement with WAAS corrections. For the mean of the 95% vertical error, there was about 60 cm improvement with CDGPS corrections and about 44 cm improvement with WAAS corrections for the ionospheric quiet day. The statistics show there was more improvement in the CDGPS corrected solution for the ionosphere-free with smoothing method on the ionospheric quiet condition day.

In the case of ionospheric storm day, there was an improvement of about 89cm with CDGPS correction and about 37cm with WAAS correction in the mean of the 95% horizontal error compared to the C1 solutions. As we expected, the improvement was more significant in the vertical component on the ionospheric storm day. It was about 1.33m with CDGPS corrections and 0.78m with WAAS corrections. However one thing clearly which we could see in the statistics was that the improvement by use of the smoothing method with WAAS corrections was more or less close to a minimal improvement compared to the improvement from CDGPS corrections.

This last result might be explained by a noise-like behavior in the WAAS fast corrections which is in addition to the local multipath and receiver noise at each station. In the case of WAAS, the resolution for the pseudorange correction (PRC), which takes into account the fast satellite clock term and the long-term satellite orbit and clock terms is 0.125m. However in the case of CDGPS, the resolution for the PRC and long-term corrections is 0.0039 m. So the low resolution of corrections behaves like noise in processing the GPS measurements with the WAAS corrections. The following Figure 10 illustrates this by means of an example.

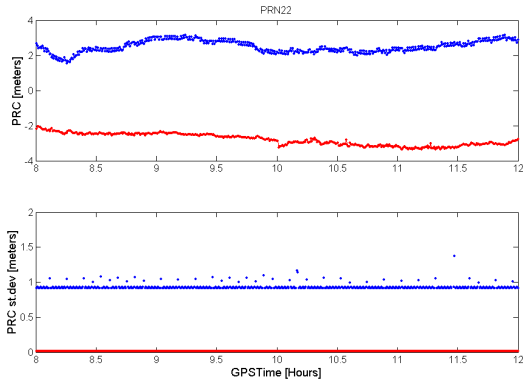

Figure 10. Upper panel shows the combined (fast and long-term) pseudorange corrections (PRC) for PRN22 during the commonly monitored time for PRN22 at the two different stations, NRC1 and PUB1 on November 10, 2004. The lower panel shows their sigma values. The blue traces show the PRC and its sigma from WAAS and the red ones represent the PRC and its sigma from CDGPS.

In Figure 10, first of all, we can see the different magnitudes of the PRC corrections between CDGPS and WAAS. The differences are due, in part, to the fact that the CDGPS uses a NAD83 (CSRS) and the WAAS uses a WGS84 as a reference frame for the satellite corrections. In the lower panel, we can see the different uncertainties for the PRC corrections. The relationship between PRC and its sigma are well described in the WAAS MOPS [1999] and CDGPS ICD [2003]. However the sigma is not a critical issue compared with the actual correction values as long as the weighted least-squares processing just counts on the relative uncertainties between satellites at a specific epoch rather than the magnitude of the uncertainties.

However we can clearly see that the WAAS PRC is noisier than the PRC from CDGPS in Figure 10.

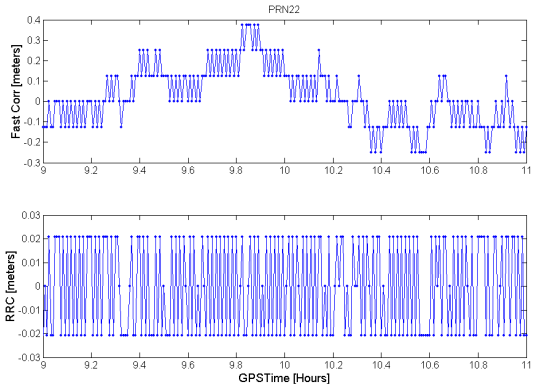

Figure 11. WAAS fast correction and range rate correction (RRC) for PRN22 on November 2004.

Finally, Figure 11 shows that the WAAS fast correction has a peck to peck variation within a specific resolution, 0.125m and we found it caused a noisy PRC correction, therefore noisy solution, for all the satellites. In the single-frequency case, we deal with about meter level accuracy. In this case, the low resolution for the corrections might be not be a significant issue. However to improve the dual-frequency precise point positing especially with WAAS corrections, it would be good to take into account the noise effect in the corrections.

CONCLUSIONS

A dual-frequency point positioning algorithm with WADGPS correction has been carefully developed, which fully takes into account the satellite clock referencing issue. To take into account the increased noise level by use of the ionosphere-free combination for the dual frequency case, we designed a modified Hatch type filter. The main advantage of this sequential forward smoother could be its utilizing the fully combined uncertainty for both systematic and random errors in the smoothing process and make use of the optimal weight into the position estimator. As long as residual biases and random errors effects could be taken into account in the GPS measurement processing with some help from the WADGPS corrections and empirical noise models as well as their uncertainties, this smoothing filter is fast, straightforward and efficient for estimating the positioning solution with WADGPS corrections.

With the developed observation model, we found about 75 cm level of improvements in the horizontal and improvements of about factor of 2 in the vertical component when the instrumental biases were taken into account. However we should note that the improvements which we saw were not only from the satellite P1-C1 bias effects but also from the combined residual effects of multipath and noise which were smoothed at the smoothing filter.

Statistics from the static testing results indicate that a few decimeter-level of positioning accuracy is attainable in 2D r.m.s. with our developed software. For these results, we didn't take into account the phase wind-up due to relative rotation of the satellite and receiver antennas, nor site displacement effects due to solid earth tides and ocean loading.

FURTHER RESEARCH

To obtain the most accurate position estimates, we need to model the solid earth tides and ocean loading and phase wind-up then should be introduced into our estimator. By estimating the residual tropospheric delays in our model, it is also possible to improve the accuracy.

Also, it might be valuable to try to smooth the WAAS pseudorange correction to follow the mean of the actual epoch-to-epoch variation. This may improve the point positioning results with WAAS corrections as long as the low resolution of corrections gives rise to a noise-like term and therefore a noisy final positioning solution.

In terms of data processing, more days and more stations need to be processed to examine the repeatability of these results, and expand the processing capabilities of this technique.

ACKNOWLEDGMENTS

Our research reported in this paper was supported by the Natural Sciences and Engineering Research Council of Cananda.and the Canada-Wide DGPS Service. The authors would like to thank to the Scripps Orbit and Permanent Array Center (SOPAC) and Geodetic Survey Division (GSD) Natural Resources Canada for providing the GPS Data.

REFERENCES

Bisnath, S.B. and R.B. Langley (2001). "High-Precision Platform Positioning with a Single GPS Receiver." Proceedings of ION GPS 2001, The Institute of Navigation, Salt Lake City, UT, U.S.A., 11-14 September, pp.2585-2593.

CDGPS ICD (2003). "GPS*C Interface Control Document (ICD) – version 3.5." Natural Resources Canada, Geodetic Survey Division, March 2003.

Chao, Y.C., S. Pullen, P. K. Enge, and B. W. Parkinson (1996). " Study of WAAS Ionospheric Integrity." Proceedings of ION GPS-96, Kansas City, MO, 17-20 September 1996, pp. 781-788.

CODE (2005): http://www.aiub.unibe.ch/ionosphere.html Accessed 21 September 2005.

Collins, J.P. and R.B. Langley (1999). "Possible Weighting Schemes for GPS Carrier Phase Observations in the Presence of Multipath." Contract report for the United States Army Corps of Engineers Topographic Engineering Center, No. DAAH04-96-C-0086/TCN 98151, March.

Gao, Y., F. Lahaye., P. Heroux., X. Liao, N. Beck., M. Olynik. (2001). "Modeling and Estimation of C1-P1 bias in GPS Receivers." Journal of Geodesy, Vol. 74, pp. 621-626.

Hatch, R. (1982), "The Synergism of GPS Code and Carrier Measurements." Proceedings of the Third International Geodetic Symposium on Satellite Doppler Positioning." DMA, NOS, Las Cruces, NM, 8-12 February, Physical Science Labortory, New Mexico State University, Las Cruces, NM, Vol. II, pp.1213-1232.

Herox, P., J. Kouba, P. Collins, and F. Lahaye (2001). "GPS Carrier-Phase Point Positioning with Precise Orbit Products." Proceeding of the International Symposium on Kinematic Systems in Geodesy, Geomatics and Navigation 2001, Banff, Alberta, Canada, 5-8 June, 2001, The University of Calgary, Calgary, Alberta, Canada.

Kee, C., T. Walter, P. Enge, and B. Parkinson (1997). "Quality Control Algorithms on WAAS Wide-Area Reference Stations." Navigation: Journal of The Institute of Navigation, Vol. 44, No. 1, Spring 1997, pp. 53-62.

McGraw, G.A, T. Murphy, M. Brenner, S. Pullen. and A.J. Van Dierendonck. (2000). "Development of the LAAS Accuracy Models." Proceeding of ION GPS 2000, Salt Lake City, UT, 19-22 September 2000, pp 1212-1223.

McGraw, G.A., Ryan S. Y. Young (2005), "Dual Frequency Smoothing DGPS Performance Evaluation Studies." Proceedings of the Institute of Navigation National Technical Meeting, The Institude of Navigation, San Diego, CA, 24-26 January, pp. 170-181.

NRCan Geodetic Survey Division (GSD) (2005): http://www.geod.nrcan.gc.ca/index_e/products_e/online_data_e/online_data_e.html Accessed 21 September 2005.

Rho, H., R.B. Langley, and A. Kassam (2003). "The Canada-Wide Differential GPS Service: Initial Performance." Proceedings of ION GPS/GNSS 2003, 16th International Technical Meeting of the Satellite Division of The Institute of Navigation, Portland, OR, 9-12 September 2003, pp. 425-436.

WAAS MOPS (1999). *Minimum Operational Performance Standards for Global Positioning System/Wide Area Augmentation System Airborne Equipment.* RTCA Inc. Documentation No. RTCA/DO-229B, 6 October, 255pp.

Zhang, Y., C. Bartone (2005). "A GPS Orbit and Clock Correction Analysis for Long Baseline High Performance DGPS." Proceeding of ION 61st Annual Meeting, Cambridge, MA, 27-29 June 2005, pp. 1062-1072.